Progress In Electromagnetics Research, Vol. 113, 47–66, 2011

MULTIFREQUENCY SELF-DIPLEXED SINGLE PATCH ANTENNAS LOADED WITH SPLIT RING RESONATORS

J. Montero-de-Paz, E. Ugarte-Muñoz and F. J. Herraiz-Martínez

Teoría de la Señal y Comunicaciones
Universidad Carlos III de Madrid
Avenida de la Universidad 30, Madrid 28911, Spain

V. González-Posadas

Ingeniería Audiovisual y Comunicaciones
Universidad Politécnica de Madrid
Carretera de Valencia km. 7, Madrid 28031, Spain

L. E. García-Muñoz and D. Segovia-Vargas

Teoría de la Señal y Comunicaciones
Universidad Carlos III de Madrid
Avenida de la Universidad 30, Madrid 28911, Spain

Abstract—In this paper, a novel approach to design multifrequency self-diplexed single patch antennas is proposed. This approach is based on a square microstrip patch antenna loaded with split ring resonators (SRRs). The working frequencies can be arbitrarily chosen and frequency ratios lower than 1.07 have been achieved. In addition self-diplexing characteristics are also achieved between transmitting and receiving ports by including SRRs in the feeding lines. Several prototypes have been manufactured and measured in the X-band showing good performance.

Received 17 December 2010, Accepted 17 January 2011, Scheduled 26 January 2011
Corresponding author: Javier Montero-de-Paz (jmontero@tsc.uc3m.es).

1. INTRODUCTION

Wireless communications systems have grown up exponentially in the recent years. Systems like mobile communications (GSM, UMTS), wireless sensor (ZigBee), personal area (Bluetooth) or wireless (WiFi) networks and radio navigation systems (GPS, Galileo) are widely used nowadays. There is a growing trend to integrate as many of these wireless systems into one single user terminal [1, 2]. In order to reduce the distortion associated to the interference from one service to another service, additional high selectivity filters are needed to achieve high isolation between both inputs. If the multifrequency antenna could highly isolate these frequencies, a great simplification in the corresponding front-end could be achieved. Thus, multifrequency (for frequencies as close as possible), compact and self-diplexed antennas will be desirable in order to reduce the overall size of the handheld device.

Microstrip patch antennas [3, 4] have been widely used in wireless communications. The most common way to obtain multifrequency performance is by adding parasitic elements with different resonant frequencies [3–8]. One possible solution to design compact multifrequency antennas with low frequency ratios could be by using metamaterial cells [9–12]. Metamaterials with simultaneously negative permittivity and permeability (Left Handed materials) have been used in microwave devices design [9, 10], or in antenna design [10–12]. Recently, dual- frequency printed dipoles were presented in [13]. Patch antennas and metamaterials have also been used together to obtain multifrequency and dual-mode patch antennas [14, 15] without increasing the size or volume of the single antenna. However, in all these previous works there was a limit on achieving arbitrarily close and different frequencies, as required for some satellite Tx/Rx services.

In addition, high isolation between ports is required in order to separate different services. Till now, not many references have appeared on isolated antennas [16–18]. All of them achieve isolation levels for orthogonal ports based on a multilayer structure or by the inclusion of multilayer defects in the substrate or in the ground structure. In [18], the idea of using filtering lines to feed the printed antenna was firstly proposed. Up to the authors' knowledge, self-diplexed patch antennas for non-orthogonal ports each of them working on different frequency bands have not been developed until now.

In this paper, the inclusion of metamaterial cells has allowed achieving high isolation self-diplexed (between not orthogonally polarized ports) multifrequency antennas based on a single patch antenna. Split ring resonators (SRRs) have been used to load both the

antenna and the filtering lines in a two layer structure in comparison with previous multilayer structures. Two or more working frequencies arbitrarily chosen can be achieved depending on the number of SRRs coupled to the patch antenna. Frequency ratios close to 1 can be achieved. Finally, a simple circuit model based on equivalent circuit and transmission line approaches is also presented.

2. ANTENNA DESIGN

Multifrequency patch antennas partially filled with left-handed (LH) structures were first presented in [14]. These antennas consisted of a conventional patch partially filled with Sievenpiper's mushrooms to achieve two ($n = -1$ and $n = +1$) or three ($n = -1$, $n = 0$ and $n = +1$) radiation modes, where n refers to the radiating mode according to the resonant condition of a patch antenna [3, 4, 14]:

$$\beta_n \cdot L = n \cdot \pi \tag{1}$$

where L is the equivalent transmission line of the patch and β_n is the propagation constant.

When the working frequencies are higher and the frequency ratio between the upper and lower frequency is close to unity (i.e., $f_{n=1}/f_{n=-1} \approx 1$) the structure proposed in [14] cannot work. This is due to the fact that working at higher and closer frequencies implies comparable dimensions between the patch and the inside mushrooms. In addition, the diameter of the vias and the gap between mushrooms must be very small, leading to sizes that are not possible to be manufactured due to physical restrictions. A study on the minimum frequency separation that can be achieved for the antennas partially filled with LH cells has been carried out on the X-band (7–12.5 GHz).

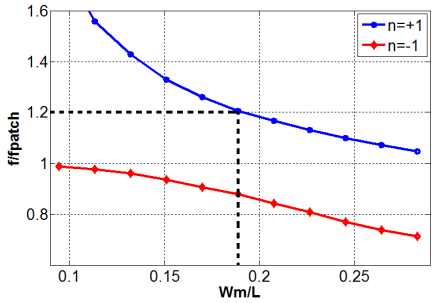

Figure 1. Ratio of the proposed antenna frequencies over the conventional isolated patch antenna frequencies vs the ratio of the inside cell length (W_m) over the patch length (L).

The minimum spacing between the gaps has been set to 0.1 mm while the minimum via diameter has been set to 0.2 mm. Figure 1 shows the normalized working frequencies (mode frequency over the isolated patch frequency) for both modes in front of the ratio between the cells length and the patch length. The minimum frequency ratio that can be achieved is 1.36 (9.8 and 7.2 GHz).

2.1. Dual-frequency Patch Antennas Loaded with SRRs

Split ring resonators are planar structures that have been widely used in metamaterials and LH structures design [9, 19–26]. They consist of a double metallic concentric rings with a width of c, separated a distance d and with a small cut on each of them at opposite sides, g. The length of the coupling side is r. In order to increase the coupling between the supporting transmission line and the corresponding SRRs, a pair of square SRRs instead of a circular one has been chosen as it is shown on Figures 2(a)–2(b). If the SRRs are excited with an orthogonal magnetic field (z-direction in Figure 2(b)) or with a parallel electric field (y-direction in Figure 2(b)) [9], they have a resonant frequency that depends on their dimensions.

First, a 2.39 mm width microstrip line on a Rogers Duroid 5880

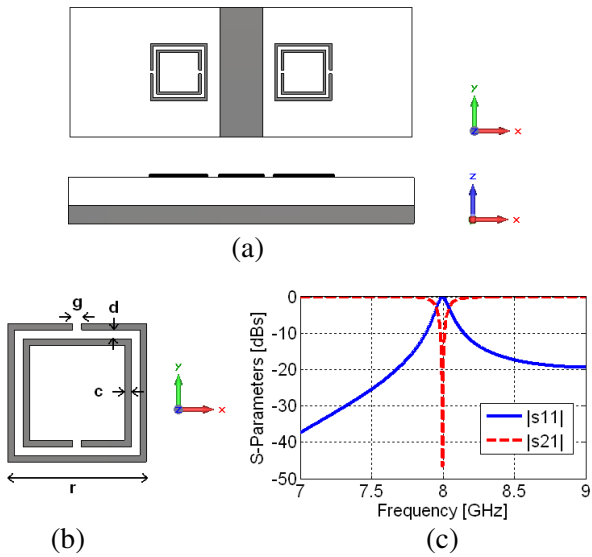

Figure 2. (a) Microstrip transmission line stop-band filter based on SRRs. (b) Single SRR. (c) Simulated S-parameter of the stop-band filter.

(with a 1.574 mm thickness) loaded with a pair of SRRs has been designed. The dimensions of the SRRs are: $r = 3.2$ mm, $c = 0.15$ mm, $d = 0.2$ mm, $g = 0.2$ mm and a gap between SRRs and Microstrip line of 0.7 mm. The resulting loaded line behaves as a notch structure that can be seen in (Figure 2(c)). These properties can be applied to a single patch antenna, due to the fact that patch antennas with resonant frequency f_o ($n = +1$ mode) can be modeled as a transmission line with length $L \approx \lambda_0/2$ and width W. The patch antenna induces, as well as a microstrip transmission line, a strong magnetic field component in the normal direction. So the same stop-band behavior obtained with a microstrip transmission line loaded with SRRs will be expected with a microstrip patch antenna loaded with SRRs.

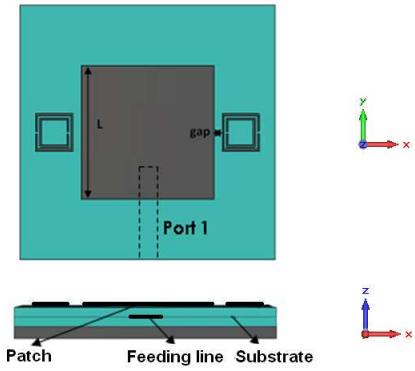

Figure 3. Sketch of the dual-frequency linear polarization patch antenna loaded with SRRs.

The proposed dual frequency antenna is shown in Figure 3. It consists of a conventional square patch antenna loaded with two equal and coplanar SRRs near the patch. The antenna parameters are the length of the patch (L) and the gap between the patch and the SRRs (gap). In addition, all the previously mentioned SRRs' parameters have to be considered. The antenna is fed through a microstrip coupled line placed beneath the patch. The dimensions of the feeding line are the length L_f and the width W_f.

Two different analyses have been undertaken to see the performance of the proposed antenna. First, if the resonant frequency of the SRRs is designed in order to fall in the patch antenna bandwidth (BW), a notch is inserted inside this bandwidth what forces two working bands (f_1 and f_3) where the frequency barrier (f_2) is the

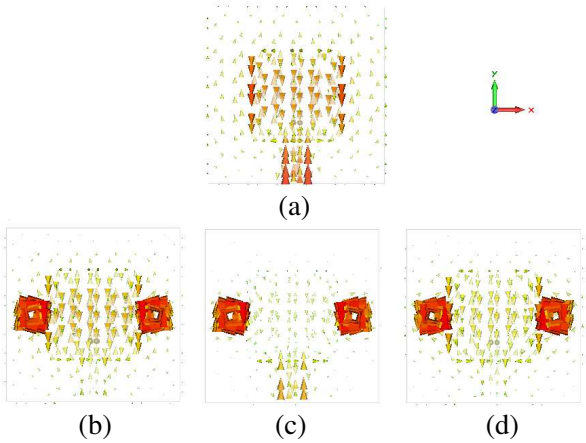

Figure 4. (a) Current density of the single patch antenna without SRRs. Current density of the patch antenna loaded with SRRs acting as a notch: (b) f_1, (c) f_2 and (d) f_3.

resonant frequency of the SRRs that is given as

$$\omega_2^2 = \frac{1}{L_S \cdot C_S} \tag{2}$$

where the inductance L_S and the capacitance C_S are the values of equivalent resonant tank circuit. The surface current density of the first configuration can be seen in Figure 4. At frequencies f_1 and f_3, a strong current is induced in the SRRs, but the currents in the patch are very similar to the ones of the patch antenna when none of the SRRs are placed next to it, thus leading to a broadside radiation pattern. On the other hand, at frequency f_2 (resonant frequency of the SRRs) almost no current is induced in the patch because the SRRs forced a negative value of the permeability (the same behavior as the stop-band filter described previously) and all energy is reflected.

Secondly, if the resonant frequency is out of the bandwidth of the patch antenna, two different working frequencies are achieved: one due to the resonance of the mode n=+1 of the patch antenna (f_1) and the other due to the self resonance of the SRRs (f_2). In the second configuration the working principle is somewhat different since a notch behavior is not possible because the resonant frequency of the SRRs is out of the unloaded single patch antenna bandwidth. In this case each working frequency is due to each resonating element (patch and SRRs). When the antenna is excited at a frequency different from the one of the patch or the SRRs, all the energy is reflected. When the antenna is excited at the resonant frequency of the patch, it accepts all the energy

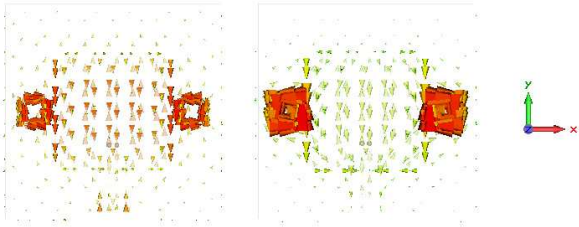

Figure 5. Current density of the single patch antenna loaded with SRRs when resonant frequency of the SRRs is not inside the BW of the unloaded patch antenna. (a) f_1 and (b) f_2.

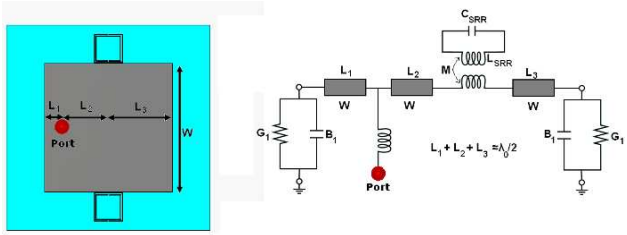

Figure 6. Lumped-element equivalent circuit model of the patch antenna loaded with SRRs.

and radiates it, leading to the field distribution of its fundamental mode (Figure 5(a)). If the exciting frequency is the one of the SRRs, they resonate and a high current along them is produced inducing, at the same time, a current in the patch similar to the fundamental mode of the patch (Figure 5(b)). This leads to a broadside radiation pattern at both frequencies.

2.2. Equivalent-circuit Model

A lumped-element equivalent circuit model for the patch antenna coupled with the SRRs is proposed in Figure 6. The patch antenna is modeled as a transmission line with length $L \approx \lambda_0/2$ (being λ_0 the wavelength corresponding to the resonant frequency of the $n = +1$ mode, f_o) and width W. The lengths of the corresponding transmission lines are indicated in both, the patch and the circuit schematic. A parallel RC circuit is put at each edge of the patch to model the radiated and the stored fields in the proximity of the patch.

The SRRs are modeled as a LC parallel tank circuit whose

resonant frequency is given by (1), where $L_S = L_{SRR}$ and $C_S = C_{SRR}$. The LC parallel tank corresponding to the SRRs is coupled to the patch through a mutual inductance, M, which models the magnetic coupling between the elements. Additional coupled LC parallel tanks must be added to the model when different SRRs are added.

CST Microwave Studio® and this equivalent circuit will be used to analyze and design the proposed antenna.

2.3. Parametric Analysis

The parametric analysis has been undertaken based on a reference square patch, 11.4 mm length with a resonant frequency of 7.67 GHz. CST Microwave Studio® will be used to study the proposed antenna. According to 1 the dependence parameters are the length of the patch (L), the coupling size of the SRRs (r), the width of the lines of the SRRs (c), the gap between the lines of the SRRs (d), the gap between the edges of the lines of the SRRs (g) and the separation between the patch and the SRRs (gap). From this analysis it can be concluded that

- When the coupling size of the SRRs (r) is increased, its resonant frequency is reduced due to the fact that the inductance L_{SRR} increases. Figure 7 shows the obtained working frequencies as a function of the length of the SRRs (r). The isolated working frequencies are shown in dashed lines while the continuous lines represent the working frequencies of the patch loaded with the SRRs. Since sometimes it is impossible to determine whether the resonance is due to the patch or the SRRs, it has been considered that the one with higher BW is due to the patch and the one with lower BW is due to the SRRs. The shadow region represents

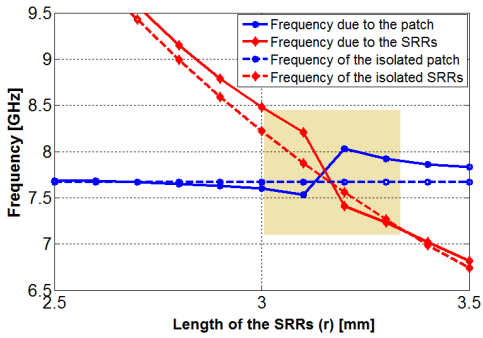

Figure 7. Proposed antenna frequencies as a function of the length of the SRRs (r). Area in yellow is the range where the SRRs behave as a notch.

the frequency band where the SRRs behave as a notch and makes possible obtain the dual frequency antenna.

- When the width of the lines of the SRRs (c) is increased, so does the resonant frequency since the value of associated inductance, L_{SRR}, gets lower.
- When the gap between the lines of the SRRs (d) enlarges, so does the frequency since the value of the associated capacitance, C_{SRR}, gets lower.
- When the gap in each SRRs (g) raises, so does the resonant frequency. This variation is very slight so it will be kept fixed.
- Finally, as the spacing between the patch and the SRRs gets larger the corresponding resonant frequencies gets closer, since the lower frequency increases while the highest frequency decreases. This can be seen in Figure 8 and is due to the decrease in the magnetic coupling, M, between the patch and the SRR. This decrease in the magnetic coupling makes the corresponding resonant frequencies get closer to the isolated resonant frequencies.

According to Figure 7, ratios lower than 1.07 can be achieved by properly designing all the previous parameters. This is an important improvement with respect to the antennas proposed in [15], as well as the fact that the antennas are completely planar. Moreover, multifrequency antennas can be obtained just by adding more SRRs with different resonating frequencies at both sides of the patch.

An interesting feature of this antenna is that when the self-resonances of the SRRs and the patch are very close (notch effect), the relative bandwidth of each of the working frequencies is very similar and depends on the position where the notch is introduced. In addition, the sum of the relative bandwidth of each frequency band

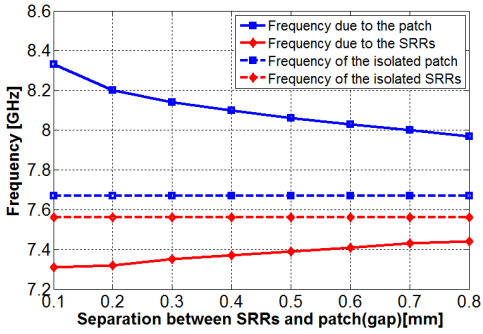

Figure 8. Proposed antenna frequencies as a function of the separation between the patch and the SRRs.

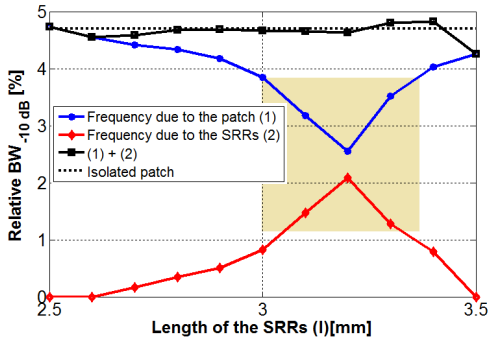

Figure 9. Relative bandwidth as a function of the length of the SRRs. Area in yellow is the range where the SRRs behave as a notch.

is approximately equal to the relative bandwidth of the unloaded patch antenna. This can be explained by making use of the corresponding loaded Q-factor. Then, the overall antenna Q-factor can be given as

$$1/Q_{antenna} = 1/Q_{patch} + 1/Q_{SRRs} \tag{3}$$

As the SRRs Q-factor is very high, the overall antenna Q-factor will be mainly given as follows

$$Q_{SRRs} \uparrow\uparrow \Rightarrow 1/Q_{antenna} \approx 1/Q_{patch} \tag{4}$$

This fact can be seen in Figure 9 (shadowed), where the working frequencies and its relative bandwidth at $-10\,\text{dB}$ is plotted as a function of the length of the SRRs (the parameter r has been chosen since it is the one that more affects to the antenna performance). Moreover, when the self resonance of the SRRs is far away from the resonance of the patch, the BW of the frequency band due to the SRRs is very narrow and the frequency band due to the patch antenna is very similar to the one of the unloaded patch.

2.4. Diplexing Characteristics

One possibility that these configurations add to patch antennas is the design of self-diplexed multifrequency antennas with non-orthogonal ports. The use of self-diplexed multifrequency antennas eliminate the necessity of using diplexers and reduce the overall number of components in transceivers systems. As a result, the efficiency is enhanced and the overall cost is reduced. Till now, all the designs of self-diplexed multifrequency patch antennas consist of orthogonal ports, each of them working on a different frequency band [16–18]. This is due to the fact that in most of the cases rectangular patches

are required in order to have one frequency associated to the electrical length of one side of the patch and other frequency associated to the electrical length of the other side of the patch. With the configuration presented in this paper, two working frequencies are achieved with no need of having rectangular patches, so self diplexed dual frequency patch antennas with non-orthogonal ports can be designed.

The aperture coupled microstrip lines [3, 4] can be a suitable feeding technique for the proposed self-diplexed antenna since it provides the maximum isolation between ports. This technique is easy to manufacture and has various degrees of freedom to get the matching [15]. In addition, the use of filtering lines instead of conventional feeding lines provides higher isolation levels between both ports, even when non-orthogonal modes are excited. Two strategies can be followed to design the filtering lines, well stop-band filtering lines rejecting the antenna's non-desired frequency, well band-pass filtering lines to allow the antenna's desired frequency.

If SRRs were coupled at both sides of a microstrip transmission line, a narrow frequency band above the SRR resonant frequency is inhibited (notch-filter explained in Section 2.1). In this way, filtering feeding lines could be obtained by adding these particles to the antenna feeding transmission lines. These lines would allow rejecting the antenna non-desired modes and improving the isolation between ports. It must be emphasized that neither the complexity nor the size of the antenna is increased. In addition the radiation parameters are kept.

The second option is to periodically insert open split ring resonators (OSRR) [26] in the filtering transmission line to achieve band-pass performance. The OSRR behaves as a series LC circuit in series with the transmission line. These particles allow obtaining band-pass filtering lines without increasing the losses very much. Two pairs of square OSRR connected to the transmission line are used. The OSSR characteristic parameters are the side of the square, r, the gap between rings, d, the width of the ring, c, the spacing between the ring and the microstrip line, *gap,* and the gap in the microstrip line e.

In this way, the self-diplexed multifrequency antenna will be composed of a patch loaded with SRRs to achieve a multifrequency performance fed with filtering lines with OSRRs to increase the isolation between transmitting and receiving ports.

3. EXPERIMENTAL RESULTS

Three different kinds of antennas have been designed and manufactured in order to prove the performance of the proposed multifrequency antennas. First, a dual frequency linearly polarized antenna is

designed, secondly a triple frequency linear polarized antenna is shown and finally a two-port self-diplexed dual-frequency antenna will be presented. For all the cases, the ratio between the working frequencies is very low achieving a 1.07 ratio.

3.1. Dual-frequency Linear Polarization with Notch Effect

The first designed, simulated and manufactured prototype is a linearly polarized dual-frequency antenna working in the X-Band at 7.66 GHz and 8.33 GHz. The dimensions of the antenna, following the Figure 2 labels, are: $L = 10.9\,\text{mm}$, $gap = 0.7\,\text{mm}$, $r = 3.2\,\text{mm}$, $c = 0.15\,\text{mm}$, $d = 0.2\,\text{mm}$ and $g = 0.2\,\text{mm}$. The chosen feeding technique is the proximity coupled microstrip line [3, 4], so two substrates are used. The chosen substrate is Rogers RT Duroid 5880 with a thickness of 0.787 mm and $\varepsilon_r = 2.2$ for both the patch substrate and the feeding line substrate. For this case the SRRs are designed to have the same resonant frequency as the patch and thus, acting as a notch. Simulations have been undertaken with CST Microwave Studio® and with the proposed equivalent circuit model. Figure 10 shows the photo of the linearly polarized manufactured antenna.

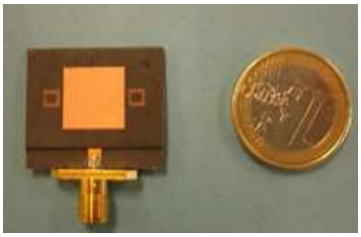

Figure 10. Manufactured dual-frequency linear polarization patch antenna loaded with SRRs acting as a notch prototype.

Reflection coefficient of the dual-frequency patch antenna loaded with SRRs has been measured and the results can be seen in Figure 11. The simulated results with CST and with the proposed equivalent circuit model are also shown in Figure 11. Good agreement is shown between the measurements and the simulations. The notch is introduced in the resonance frequency of the SRRs. It can also be appreciated that the sum of both frequency bands are quite close to the relative BW of the unloaded patch antennas as explained in Section 2.3.

Table 1 summarizes the results of both the simulation and measurements. A slight change in the relative BW at $-10\,\text{dB}$ can be appreciated. This can be the result of a little change in the SRRs

Table 1. (a) Microstrip transmission line stop-band filter based on SRRs. (b) Single SRR. (c) Simulated S-parameter of the stop-band filter.

Simulation		Measurement	
Frequency	Relative $BW_{-10\,dB}$	Frequency	Relative $BW_{-10\,dB}$
7.67 GHz	1.96%	7.71 GHz	2.33%
8.30 GHz	2.53%	8.33 GHz	1.68%

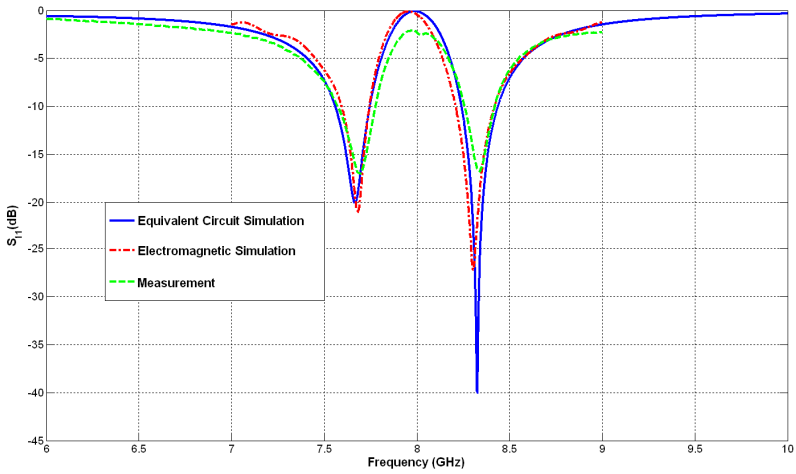

Figure 11. Measured reflection coefficients of the proposed dual-frequency linearly polarized antenna with a notch effect antenna.

dimensions, thus leading to a slight change in its resonant frequency (small shift of the notch frequency position). With this prototype a frequency ratio between both working frequencies is 1.087.

Finally, the measured radiation patterns are shown in Figure 12. The obtained radiation patterns are broadside at both frequencies and the cross polarization component presents reasonable values. Then, for both frequencies the cross polarization component is lower than 22 dB for the main beam direction.

3.2. Triple-frequency with Linear Polarization

The second designed, simulated and manufactured prototype is a triple-frequency antenna with linear polarization working in the X-Band at 7.26 GHz, 7.48 GHz and 8.09 GHz. For this case, a third set of SRRs has been included to introduce a third resonant frequency. The

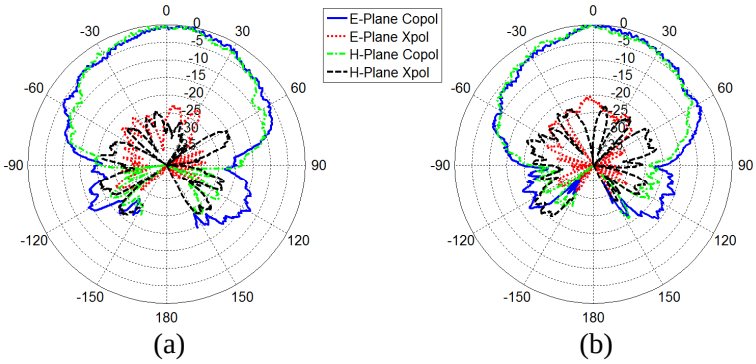

Figure 12. Measured radiation pattern of the dual-frequency patch antenna loaded with SRR: (a) 7.67 GHz and (b) 8.33 GHz.

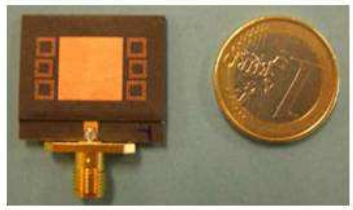

Figure 13. Manufactured triple-frequency linear polarization patch antenna loaded with SRRs prototype.

dimensions of the proposed prototype are $L = 11.3\,\text{mm}$, central SRRs: $gap = 1.2\,\text{mm}$, $r = 3.4\,\text{mm}$, $c = 0.15\,\text{mm}$, $d = 0.2\,\text{mm}$, $g = 0.2\,\text{mm}$; top and bottom SRRs: $gap = 0.8\,\text{mm}$, $r = 3.3\,\text{mm}$, $c = 0.15\,\text{mm}$, $d = 0.2\,\text{mm}$, $g = 0.2\,\text{mm}$. The separation between SRRs is 0.7 mm. The manufactured prototype is shown in Figure 13 and the simulated and measured results are shown in Figure 14 and Table 2. Once again it can be emphasized that the agreement between electromagnetic simulation, equivalent circuit simulation and measurements is great, despite a small shift in the resonant frequency of the notches which leads to a variation in the relative bandwidth. It must also be noted that the resonant frequencies can be arbitrarily chosen and the ratio between any pair of them is different.

The measured radiation patterns at the three working frequencies are shown in Figure 15. Radiation obtained at the three frequencies is broadside type and very similar to a conventional patch one. The cross polarization component presents reasonable values. Then, for the three frequencies the cross polarization component is lower than 20.5 dB in the main beam direction.

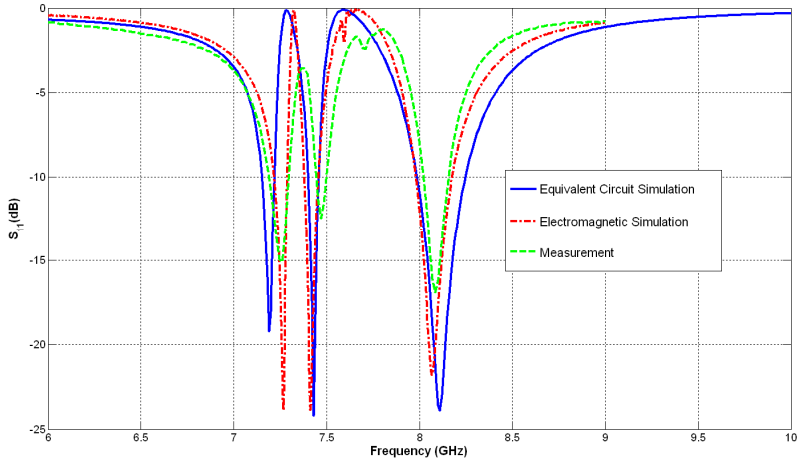

Figure 14. Measured and simulated reflection coefficients of the triple-frequency patch antenna loaded with SRRs. The simulations have been carried out with an electromagnetic simulator (CST Microwave Studio) and the proposed equivalent circuit model.

Table 2. Reflection coefficients of the triple-frequency antenna.

Simulation		Measurement	
Frequency	Relative $BW_{-10\,dB}$	Frequency	Relative $BW_{-10\,dB}$
7.25 GHz	0.87%	7.26 GHz	1.47%
7.45 GHz	1.11%	7.48 GHz	0.71%
8.10 GHz	2.48%	8.09 GHz	1.68%

3.3. Self-diplexed Multifrequency Antenna

The self-diplexed multifrequency antenna designed, simulated and manufactured prototype can be seen in Figure 16. It consists of a dual frequency patch antenna loaded with SRRs feeded by two aperture-coupled microstrip lines [3, 4]. The dimensions of the antenna, following the labels of Figure 2(b) and Figure 3, are $L = 11.4$ mm, $gap = 0.4$ mm, $r = 3.7$ mm, $c = 0.3$ mm, $d = 0.3$ mm, $g = 0.35$ mm. As substrate for the patch antenna Rogers RT Duroid 5880 with $\varepsilon_r = 2.2$ and $h = 0.787$ mm has been chosen. Two slots were made in the ground plane in order to feed the patch antenna. Their dimensions are 6 mm long and 0.3 mm width and they are 3.85 mm away from the center of the patch. OSRRs [26] were placed on each microstrip line in order to behave as pass-band filtering lines. The dimensions of the OSRRs

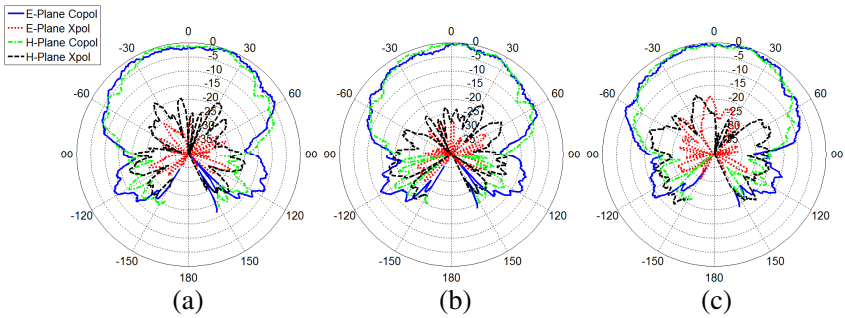

Figure 15. Measured radiation pattern of the triple-frequency patch antenna loaded with SRR: (a) 7.25 GHz, (b) 7.45 GHz and (c) 8.10 GHz.

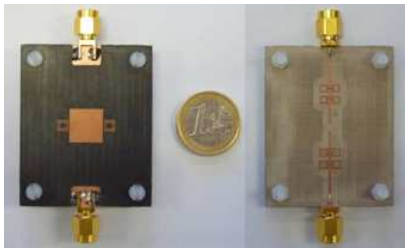

Figure 16. Manufactured dual-frequency same polarization self-diplexed patch antenna proposed. Front and back view.

Table 3. S-parameters of the self-diplexed multifrequency antenna.

Measurement			
Frequency	$\|S_{11}\|$	$\|S_{21}\|$	$\|S_{22}\|$
7.77 GHz	−18.83 dB	−32.61 dB	−0.93 dB
8.695 GHz	−0.91 dB	−29.56 dB	−20.43 dB

placed in the 50 Ω microstrip lines are: $r_1 = 3.1$ mm, $c_1 = 0.2$ mm, $d_1 = 0.3$ mm, $gap_1 = 0.35$ mm and $e_1 = 0.3$ mm; $r_2 = 2.84$ mm, $c_2 = 0.2$ mm, $d_2 = 0.3$ mm, $gap_2 = 0.35$ mm and $e_2 = 0.3$ mm. Separation between OSRRs is 4.1 mm and 3.84 mm respectively. The chosen substrate for the feeding lines is Arlon 600 with $\varepsilon_r = 6$ and $h = 0.6$ mm.

The simulated and measured S-parameters can be seen in Figure 17 and Table 3. With this configuration, isolation levels around 30 dB in both frequency bands were obtained between ports. A small

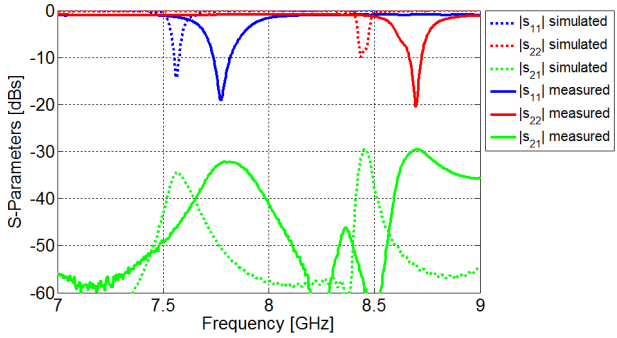

Figure 17. Simulated (dashed-line) and measured S-parameters of the self-diplexed dual-frequency patch antenna.

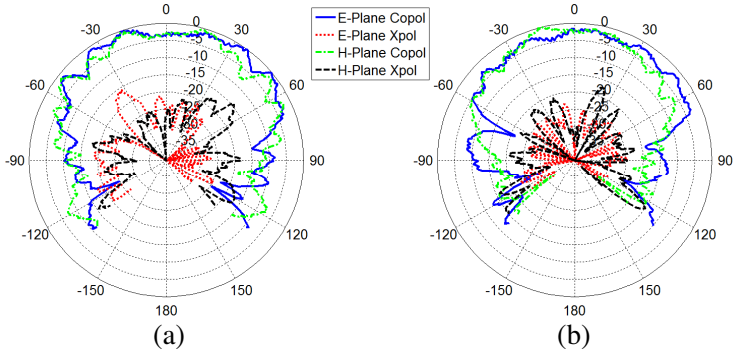

Figure 18. Measured radiation pattern of the manufactured self-diplexed dual-frequency patch antenna: (a) Port 1 (lower frequency) and (b) Port 2 (higher frequency).

frequency shift between simulation and measurements can be observed due to the manufacture process. The machine has eroded some substrate around the feeding lines (as can be seen on Figure 16, back view) which translates into a reduction of the feeding lines substrate's effective permittivity. As a consequence, the resonance shifts to higher frequencies.

The measured radiation patterns at the working frequencies on each port are shown in Figure 18. Radiation obtained at the working frequency of each port is broadside type and very similar to a conventional patch one. The cross polarization component presents reasonable values.

4. CONCLUSION

Multifrequency patch antennas loaded with SRRs have been presented. Dual-frequency antennas with arbitrarily chosen working frequencies have been designed. These antennas reduce the overall size of current multifrequency patch antennas solutions as long as the ratio of the working frequencies, which can be chosen as close as desired. Ratios of less than 1.07 were achieved. Moreover, multifrequency antennas with more than two working frequencies can be also designed just by adding more SRRs.

Also a study on the bandwidth behavior of these antennas and a simple circuit-model has been presented. Results obtained in measurements and with electromagnetic simulations agree with the ones obtained with the equivalent-circuit model presented here.

In addition, the self-diplexion with non-orthogonal ports capabilities of these antennas were explored and different configurations were proposed.

Finally, three manufactured prototypes have been presented: a dual-frequency linear polarization patch antenna, a triple-frequency linear polarization patch antenna and a self-diplexed multifrequency patch antenna. The first and second antennas have a relative bandwidth at -10 dB close to 2% and a broadside radiation pattern similar to the one of a conventional patch antenna at each working frequency. Moreover the self-diplexed antenna has isolation levels between non-orthogonal ports around 30 dB.

REFERENCES

1. "Special issue on multifunction antennas and antenna systems," *IEEE Transactions on Antennas and Propagation*, Vol. 54, No. 2, 2006.
2. Martínez-Vázquez, M., O. Litschke, M. Geissler, D. Heberling, A. M. Martínez-González, and D. Sánchez-Hernández, "Integrated planar multiband antennas for personal communication handsets," *IEEE Transactions on Antennas and Propagation*, Vol. 54, No. 2, 2006.
3. Garg, R., P. Barthia, I. Bahl, and A. Ittipiboon, *Microstrip Design Handbook*, Artech House, 2000.
4. James, J. R. and P. S. Hall, *Handbook of Microstrip Antennas*, Peter Peregrinus, London, 1989.
5. Heidari, A. A., M. Heyrani, and M. Nakhkash, "A dual-band circularly polarized stub loaded microstrip patch antenna for GPS

applications," *Progress In Electromagnetics Research*, Vol. 92, 195–208, 2009.

6. Wang, E., J. Zheng, and Y. Liu, "A novel dual-band patch antenna for WLAN communication," *Progress In Electromagnetic Research C*, Vol. 6, 93–102, 2009.
7. Mishra, A., P. Singh, N. P. Yadav, J. A. Ansari, and B. R. Vishvakarma, "Compact shorted microstrip patch antenna for dual-band operation," *Progress In Electromagnetics Research C*, Vol. 9, 171–182, 2009.
8. Maci, S. and G. Biffi Gentili, "Dual-frequency patch antennas," *IEEE Antennas and Propagation Magazine*, Vol. 39, No. 6, 1997.
9. Marqués, R., F. Martín, and M. Sorolla, *Metamaterials with Negative Parameters*, John Wiley & Sons, Hoboken, NJ, 2007.
10. Caloz, C. and T. Itoh, *Electromagnetic Metamaterials: Transmission Line Theory and Microwave Applications*, Wiley, New York, 2004.
11. Engheta, N. and R. W. Ziolkowski, *Metamaterials: Physics and Engineering Explorations*, Wiley-IEEE Press, August 2006.
12. Eleftheriades, G. V. and K. G. Balmain, *Negative-refraction Metamaterials: Fundamental Principles and Applications*, Willey-IEEE Press, July 2005.
13. Herraiz-Martínez, F. J., L. E. García-Muñoz, D. González-Ovejero, V. González-Posadas, and D. Segovia-Vargas, "Dual-frequency printed dipole loaded with split ring resonators," *IEEE Antennas and Wireless Propagation Letters*, Vol. 8, 2009.
14. Herraiz-Martinez, F. J., V. Gonzalez-Posadas, L. E. García-Muñoz, and D. Segovia-Vargas, "Multifrequency and dual patch antennas partially filled with left-handed structures," *IEEE Trans. on Antennas and Propagation,* Vol. 56, No. 8, 2527–2539, 2008.
15. Herraiz-Martinez, F. J., E. Ugarte-Muñoz, V. Gonzalez-Posadas, L. E. García-Muñoz, and D. Segovia-Vargas, "Self-diplexed patch antennas based on metamaterials for active RFID systems," *IEEE Trans. on Microwave Theory and Techniques*, Vol. 57, No. 5, Part 2, 1330–1340, 2009.
16. Barba, M., "A high-isolation, wideband and dual-linear polarization patch antenna," *IEEE Trans. on Antennas and Propagation,* Vol. 56, No. 5, 1472–1476, 2008.
17. Sim, C. D., C. C. Chang, and J. S. Row, "Dual-feed dual-polarized patch antenna with low cross polarization and high isolation," *IEEE Trans. on Antennas and Propagation,* Vol. 57, No. 10, 3405–3409, 2009.

18. Chung, Y., S. S. Jeon, S. Kim, D. Ahn, J. I. Choi, and T. Itoh, "Multifunctional microstrip transmission lines integrated with defected ground structure for RF front-end application," *IEEE Trans. on Microwave Theory and Techniques*, Vol. 52, No. 5, 1425–1432, 2004.
19. Andres-Garcia, B., L. E. Garcia-Munoz, V. Gonzalez-Posadas, F. J. Herraiz-Martínez, and D. Segovia-Vargas, "Filtering lens structure based on SRRs in the low THz band," *Progress In Electromagnetic Research*, Vol. 93, 71–90, 2009.
20. Kim, D.-O., N.-I. Jo, H.-A. Jang, and C.-Y. Kim, "Design of the ultrawideband antenna with a quadruple-band rejection characteristics using a combination of the complementary split ring resonators," *Progress In Electromagnetics Research*, Vol. 112, 93–107, 2011.
21. Duan, Z., S. Qu, and Y. Hou, "Electrically small antenna inspired by spired split ring resonators," *Progress In Electromagnetics Research Letters*, Vol. 7, 47–57, 2009.
22. Kim, D.-O., N.-I. Jo, D.-M. Choi, and C.-Y. Kim, "Design of the ultra-wideband antenna with 5.2 GHz/5.8 GHz band rejection using rectangular split-ring resonators (SRRs) loading," *Journal of Electromagnetic Waves and Applications*, Vol. 23, No. 17–18, 2503–2512, 2009.
23. Liu Y., X. Chen, and K. Huang, "A novel planar printed array antenna with SRR slots," *Journal of Electromagnetic Waves and Applications*, Vol. 24, No. 16, 2155–2164, 2010.
24. Monti, G. and L. Tarricone, "Negative group velocity in a split ring resonator-coupled microstrip line," *Progress In Electromagnetic Research*, Vol. 94, 33–47, 2009.
25. Baena, J. D., J. Bonache, F. Martín, R. Marqués Sillero, F. Falcone, T. Lopetegi, M. A. G. Laso, J. García-García, I. Gil, M. Flores Portillo, and M. Sorolla, "Equivalent-circuit models for split-ring resonators and complementary split-ring resonators coupled to planar transmission lines," *IEEE Trans. on Microwave Theory and Techniques*, Vol. 53, No. 4, 1451–1461, 2005.
26. Martel, J., J. Bonache, R. Marqués, F. Martín, and F. Medina, "Design of wide-band semi-lumped bandpass filters using open split ring resonators," *IEEE Microwave and Wireless Components Letters*, Vol. 17, No. 1, January 2007.